**Program Digest, 2019 IEEE International Ultrasonics Symposium (IUS)**
**Glasgow, Scotland, October 6-9, 2019**

# Improving ultrasonic medical image quality by attenuation of the secondary lobes

Oscar Martínez-Graullera *Member, IEEE* *, Virginia Yagüe-Jiménez*, Montserrat Parrilla Romero*
and Alberto Ibáñez Rodríguez *
* Inst. Tecnologías Físicas y de la Información. Spanish National Research Council (CSIC),
C/ Serrano 144, Madrid 28006, Spain
Email: oscar.martinez@csic.es

***Abstract*—In ultrasound imaging, the delay-and-sum beamforming constitutes a solid measure of the acoustic reflectivity of the scene. If it is applied to synthetic images following the Total Focus Method, it can generate an image with high resolution and contrast. The present work analyzes the data set that composes an image point from a statistical point of view and proposes a new beam formation technique capable of improving the contrast and resolution of the image.**

***Index Terms*—beamforming, Rician distribution, medical imaging**

## I. Introduction

Along the last decade the increase of the computational power has popularized the appearance of beamforming solutions based on Full Matrix Capture (FMC) acquisition strategy. The most popular beamforming technique for this set of data is the Delay and Sum (DAS) that is integrated in the Total Focusing Method (TFM) to generate fully focused images [1].

For a point in the Region Of Interest (ROI), the DAS-TFM is implemented as the sum of the FMC signal samples that accomplish the focusing law. This operation provides a robust measure of the scene reflectivity and it is able to generate a very high resolution image. However, the true potential of the information contained in the FMC is underutilized by the DAS.

In particular, it is interesting to analyze how the spatial distribution of the received samples is organized in the coarray and how secondary lobes are composed. With this information it is possible to develop processing techniques oriented to avoid its formation or at least to reduce its influence in the image. The work presented here is addressed to solve this question in linear array.

## II. Estimate of the reflectivity

### A. Delay and Sum Beamforming

Let's define the set $\text{FMC}(\vec{x})$ as the collection of samples used to compute the reflectivity at the point $\vec{x}$ of the ROI obtained with a linear array of $N$ elements.

$$\text{FMC}(\vec{x}) : \left\{ s_{ij}(\tau), \tau = \left|\frac{\vec{x}-\vec{x}_i}{c}\right| + \left|\frac{\vec{x}-\vec{x}_j}{c}\right| \forall i,j=[1,N] \right\} \quad (1)$$

This work has been supported by the AEI/FEDER (EU). Project DPI2016-80239-R

where $\vec{x}_i$ and $\vec{x}_j$ are emitter and receiver positions respectively. The value used to evaluate at $\vec{x}$ the corresponding reflectivity of the ultrasonic imaging by the DAS beamforming is the summation of all the $\text{FMC}(\vec{x})$ set.

For convenience, we can assume that each sample at $\text{FMC}(\vec{x})$ is composed by the reflectivity $m_{ij}(\vec{x})$ at that point and a noise term $n_{ij}(\tau)$ that includes thermal noise and all the acoustic information that is not related with the point $\vec{x}$:

$$s_{ij}(\tau) = m_{ij}(\vec{x}) + n_{ij}(\tau) \simeq m(\vec{x}) + n_{ij}(\tau) \quad (2)$$

where $m(\vec{x})$ is a value representative of the reflectivity at $\vec{x}$ that is in common for all the emission-reception transducer pairs.

The DAS beamforming provides an estimate of the reflectitivity as:

$$\hat{m}(\vec{x}) = \left| m(\vec{x}) + \sum_{i=1}^{N}\sum_{j=1}^{N} \frac{n_{ij}(\tau)}{N^2} \right| = |m(\vec{x}) + n(\vec{x})| \quad (3)$$

This value is coincident with $m(\vec{x})$ if $n(\vec{x})$ is equal to zero. Unfortunately, this condition is difficult to accomplish when the acoustic nature of $n(\vec{x})$ is representative in $\vec{x}$. Therefore, to improve the estimate, our objective is to minimize the term $n(\vec{x})$. However, the acoustic noise is determined by the ROI, that is invariant between acquisitions. So, there is a lack of diversity that makes difficult to apply conventional strategies. The solution addressed in this paper is to induce the diversity by applying changes in the acquisition system. As far as we are concerned, this scenario can be generated via virtual sparse arrays.

Sparse arrays are configured by the random selection of active elements in the aperture [2]. In this sense, each sparse configuration is able to provide its own estimate of the reflectivity of the ROI. This estimate is almost coincident at the position but differs in the region where secondary lobes are located. In Figure 1, it can be seen two examples for an array of 16 elements, where each green squares are active elements and blue squares are no-active. Each aperture has its own sidelobes distribution. Based on this fact, we are able to develop a sample space if the signals of the $\text{FMC}(\vec{x})$ are conveniently combined in virtual sparse configurations.

 

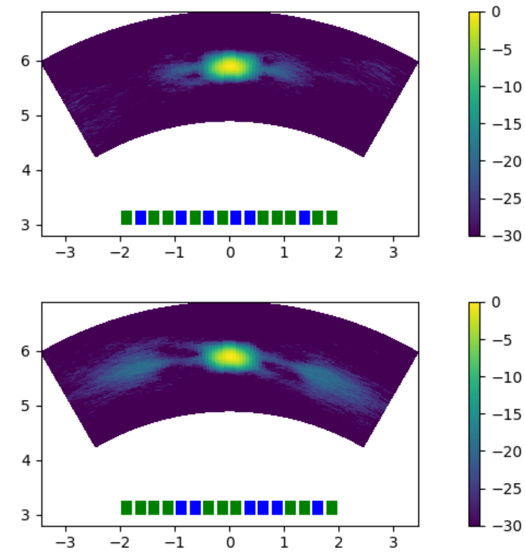

Fig. 1. Two examples of sparse array. Image of a reflector produced by the active green elements

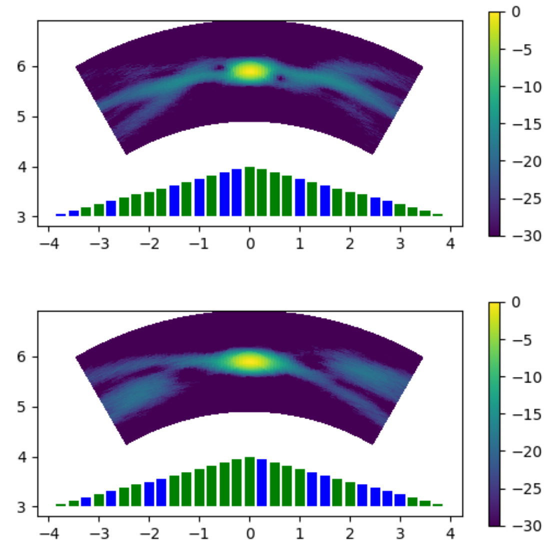

Fig. 2. Two examples of sparse coarray. Image of a reflector produced by the active green elements

### B. Generation of the sample space in the coarray

The coarray [3] is a mathematical tool that is obtained by the spatial convolution of emission, $E[n]$, and reception aperture, $R[n]$.

$$C[n] = E[n] * R[n] \tag{4}$$

We redefine FMC($\vec{x}$) in the coarray domain by grouping the signals according to their spatial frequency as $n = i + j$. Then,

$$\text{FMC}(\vec{x})[n]: \quad \left\{ c[n] = \sum_{n=1}^{2N-1} s_{ij}(\tau), \quad i + j = n \right\} \\ \forall \quad s_{ij}(\tau) \in \text{FMC}(\vec{x}) \tag{5}$$

The concept of sparse arrays can also be applied to the coarray. Sparse arrays approach can be applied in the coarray domain, selecting random active spatial frequencies. Each sparse configuration is also able to provide an alternative map of the reflectivities of the ROI. In Figure 2, two examples of sparse coarrays are represented by a triangular shape. As in the case of Figure 1, secondary lobes show different spatial distribution.

We define $\mathbf{C}$ as a random set of $N_c$ elements of the $[1, 2N-1]$ spatial frequencies that compose the coarray. Consequently, the reflectivity estimate is determined by:

$$\hat{m_c}(\vec{x}) = \left| \sum_{n=1}^{2N-1} \frac{c[n]}{N_p} \right|, \qquad n \in \mathbf{C} \tag{6}$$

$$= \left| m(\vec{x}) + \sum_{i=1}^{N} \sum_{j=1}^{N} \frac{n_{ij}(\tau)}{N_p} \right|, \quad i + j \in \mathbf{C} \tag{7}$$

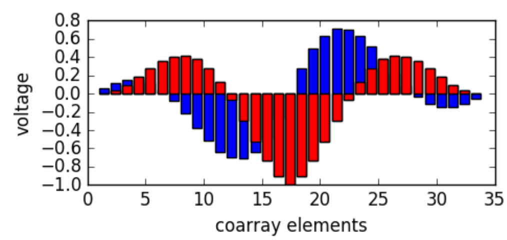


Fig. 3. Distribution of the values of samples FMC($\vec{x}$)$[n]$ (I blue, Q red) in the coarray distribution in a position $\vec{x}$ corresponding to the 1st secondary lobe.

where $N_p$ is the number of signals involved in this particular $\mathbf{C}$ set.

In order to determine the degree of sparsity suitable for this scenario, the shape of the first sidelobe coarray projection is considered. In Figure 3 phase and quadrature signal samples are represented along the coarray. In this particular case an oscillation of $1.5\lambda$ is produced in the coarray. Therefore, to reduce the sidelobe level we have chosen:

$$N_c = \frac{2}{3}(2N - 1) \tag{8}$$

Then, if a large enough number of $\mathbf{C}$ cases is considered an histogram of estimates can be constructed. In Figure 4 this histogram, composed by $N_r = 100000$ cases, is presented for the first sidelobe position. The DAS estimate is also indicated with a black line. The histogram presented follows a Rician distribution. Due to the nature of the scenario, this is analogue to a multipath problem [4]. Furthermore, Rician distribution is frequently used to study textures in ultrasonic medical images [5]–[7]. The DAS estimate is precisely another value contained in the distribution support.

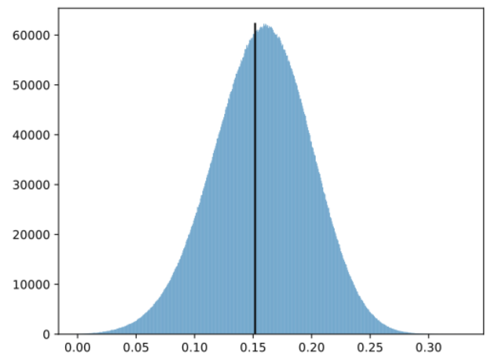


Fig. 4. Distribution of estimates of the reflectivity in the first lobe position. The DAS estimate is presented with a black line.

### C. Rician beamforming

Due to the shape of the histogram follows the Rician distribution, the set of all possible estimates can be modelled by the equation:

$$f(y|\nu,\sigma) = \frac{y}{\sigma^2}\exp\left(\frac{-(y^2+\nu^2)}{2\sigma^2}\right) I_0\left(\frac{y\nu}{\sigma^2}\right) \tag{9}$$

where $\nu$ and $\sigma$ are the characteristic parameters of the distribution [8]. Although all image points follow the Rician distribution, we can identify that there are three representative cases. The first one corresponds with a position of a reflector. In this case, the distribution converges to a Normal distribution with low variance and high mean (see Figure 5 top). The second case corresponds to a position where thermal noise is significant. In this case, the distribution converges to a Rayleigh distribution (see Figure 5 bottom). The third case corresponds with a position where acoustic noise is significant. In this case, the left slope is slower than the right one and its shape tends to the Rician distribution (see Figure 4).

Now, our estimate of reflectivity, $\hat{m}_p(\vec{x})$ is obtained directly from the Rician distribution using a percentile. For the case of the medical image, where to evaluate the image the texture is important, we use the corresponding Cumulative Distribution Function (CDF) $F(y)$. From this function we obtain the probability of our initial estimate $F(\hat{m}(\vec{x}))$. Then, we reduce this probability by means of

$$\hat{m}_p(\vec{x}) = F^{-1}(pF(\hat{m}(\vec{x}))) \tag{10}$$

## III. Experimental Results

In order to evaluate the performance of the proposed beamformer, a 64 element arrays (2.5 MHz, Vermon$^{\text{TM}}$) has been used to acquire the FMC of a phantom CIRS$^{\text{TM}}$ (model 040GSE). Therefore, for each point of the ROI, the $\hat{m}(\vec{x})$ of full array and a the $\hat{m}_c(\vec{x})$ values corresponding to a set $N_r = 100000$ sparse coarrays has been computed. Each image point is characterized by the DAS and by the $\nu$ and $\sigma$ values corresponding to the fitted Rician distribution. The

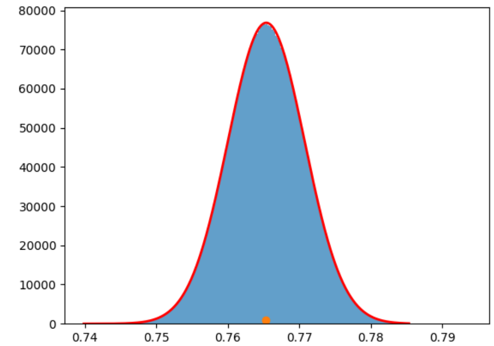


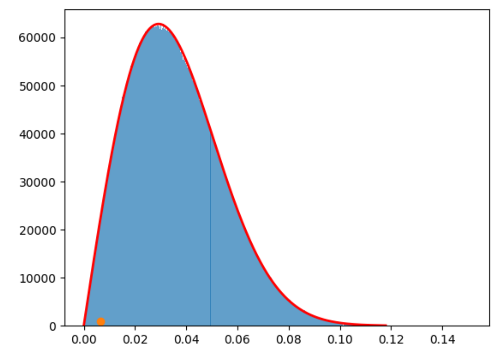


Fig. 5. Top: distribution of $\hat{m}_c(\vec{x})$ where a reflector is dominant. Bottom: distribution of $\hat{m}_c(\vec{x})$ where thermal noise is dominant. The red point represents the $\hat{m}(\vec{x})$ value and the red line the Rician distribution evaluated from the histogram

percentile which corresponds with this DAS value is obtained and modified by the factor ($p = 0.1$). The estimation is computed by the CDF, of this percentile, which is used as the new reflectivity value.

In Figure 6 the corresponding DAS image is presented. In Figure 7 we can see the improvement achieved by the Rician Beamforming. It can be seen how the contrast in the image has been increased.

In order to evaluate the real improvement, Figure 8 presents the linear value of $\hat{m}(\vec{x}) - \hat{m}_{0.1}(\vec{x})$. The image shows how the proposed method reduces secondary lobes. In particular the value of $N_c$ helps to reduce the influence of the first secondary lobes.

## IV. Conclusions

The results show that the Rician beamformer is able to increase the contrast in the image. The experimental results show the validity of the proposed method in real measurements.

Future works will be addressed to improve the analysis of the distribution in order to unmask the reflector in regions where noise is significant. In this sense, it is specially interesting where the acoustic noise is more relevant.

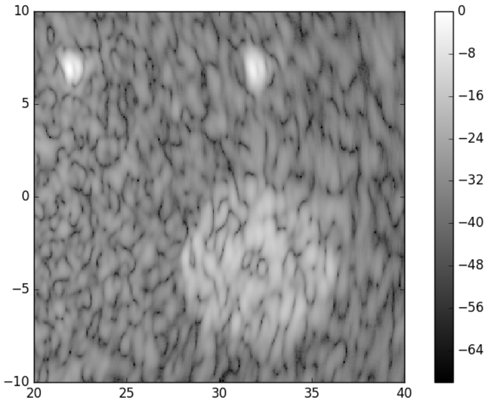


Fig. 6. Delay and Sum Beamforming.

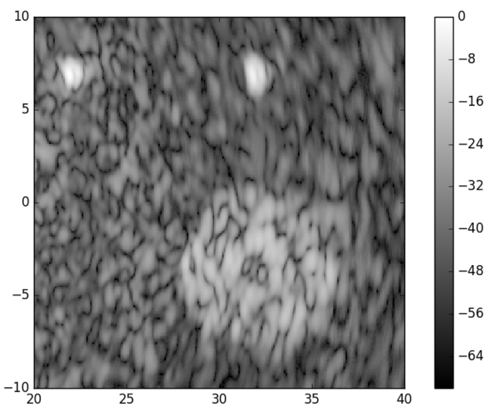


Fig. 7. Rician Beamforming $\hat{m}_{0.1}(\vec{x})$.

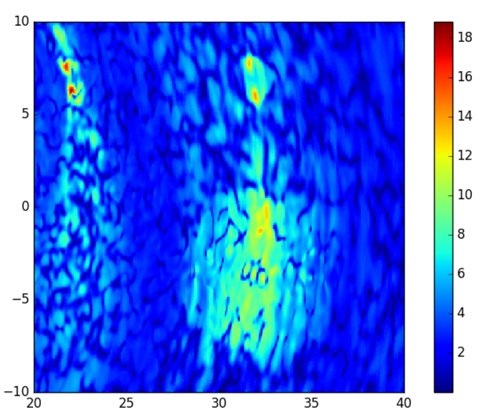


Fig. 8. Linear value of $\hat{m}(\vec{x}) - \hat{m}_{0.1}(\vec{x})$

## References

[1] C. Holmes, B. W. Drinkwater and P. D. Wilcox, “Post-processing of the full matrix of ultrasonic transmit–receive array data for non-destructive evaluation”, NDT & E Int., 38(8) 2005, 701 – 711.

[2] G.R. Lockwood, et al, ”Optimizing the radiation pattern of sparse periodic linear arrays”, IEEE Trans. on UFFC, 43(1), 1996, 7-14.

[3] R. T. Hoctor and S. A. Kassam, “The unifying role of the coarray in aperture synthesis for coherent and incoherent imaging”, Proceedings of the IEEE, vol. 78, no 4, 1990, 735-752.

[4] Bernard Sklar, “Rayleigh Fading Channels in Digital Communication Systems Part I: Characterization”, IEEE Communication Magazine, July 1997, 90–100.

[5] Aysal, Tuncer C., and Kenneth E. Barner. ”Rayleigh-maximum-likelihood filtering for speckle reduction of ultrasound images”. IEEE Transactions on Medical Imaging, 26.5 2007, 712-727.

[6] Nadarajah, Saralees. ”Statistical distributions of potential interest in ultrasound speckle analysis”, Physics in Medicine & Biology, 52(10), 2007, 213-227.

[7] Eltoft, T. ”Modeling the amplitude statistics of ultrasonic images”. IEEE Transactions on Medical Imaging, 25.2 2006, 229-240.

[8] Kushal K. Talukdar, William D. Lawing. “Estimation of the parameters of the Rice distribution”. J. Acoust. Soc. Am. 89 (3), 1991, 1193-1197.